Low Temperature Physics/Fizika Nizkikh Temperatur, 2020, vol. 46, No. 12, pp.

Low-temperature luminescence of ScF_3 single crystals under excitation by VUV synchrotron radiation

Viktorija Pankratova, Juris Purans, and Vladimir Pankratov

Institute of Solid State Physics, University of Latvia, Riga LV-1063, Latvia
E-mail: vladimirs.panktatovs@cfi.lu.lv

Received July 9, 2020, published online October 21, 2020

Photoluminescence and excitation spectra of ScF_3 single crystals have been measured under vacuum ultraviolet excitations utilizing undulator synchrotron radiation from 1.5 GeV storage ring of MAX IV synchrotron. The emission peak at 280 nm is explained as emission band of self-trapped excitons in ScF_3. This emission is quenched at 50 K and activation energy of thermal quenching was obtained. The excitation spectrum in vacuum ultraviolet spectral range exhibits that the luminescence of self-trapped excitons effectively occurs under direct excitation in the excitonic absorption band, whereas under higher energies this excitation is strongly suppressed, however multiplication of electronic excitation processes have been successfully identified.

Keywords: ScF_3, VUV luminescence spectroscopy, synchrotron radiation.

1. Introduction

Scandium fluoride (ScF_3) is a wide-bandgap material belonging to perovskite-type compounds [1]. ScF_3 demonstrates strong negative thermal expansion (NTE) [2], which is more pronounced than that of most known NTE materials. Therefore, intensive studies of the NTE phenomenon in ScF_3 by means of both experimental and theoretical approaches have been reported during recent years [3–6]. Nevertheless, optical and luminescence properties of ScF_3 are poorly studied so far. These experimental data are important for the understanding of the electronic structure of this material. Taking into account that luminescence method is very sensitive to lattice structure and symmetry changes, the study of intrinsic luminescence properties can be extremely important for dipper understanding and analysis of NTE in ScF_3. Luminescence studies of ScF_3 reported in the literature are focused on the luminescence of extrinsic centers mainly rare-earth ions [7–9].

ScF_3 belongs to the class of wide bandgap materials. One of the most common intrinsic luminescence centers in such materials is a self-trapped exciton (STE) [10–13]. Systematic studies of STE luminescence was started in the middle of the 20 century. The main reason of high interest to STE luminescence was driven by the investigations of radiation effects/defects in wide-bandgap materials, mainly alkali halides [14, 15]. It was clearly demonstrated that non-radiative relaxation of STE, which is a competing relaxation channel to STE luminescence, leads to the formation of radiation defects in alkali halides [10]. Later on, luminescence of STE was intensively studied in other compounds like condensed rare-earth gases, alkali-earth fluorides, silver halides, chalcogenides, silicon dioxide, etc. [10 and references therein]. Furthermore, STE luminescence was also detected and studied in LaF_3 [16] and YF_3 [17, 18] which are belong to trifluoride compounds as well as ScF_3 are.

Since the excitons in wide-bandgap materials are in the deep ultraviolet and vacuum ultraviolet (VUV) spectral ranges, synchrotron radiation has proved especially useful in excitation spectroscopy [19–28]. For instance, it was shown [29] that in alkali halides the excitation spectra in VUV range exhibit general correlation between peaks in fundamental optical absorption and dips in luminescence yield, attributable in part to reflection of the excitation light, genuine state-selectivity controlling subsequent STE relaxation path, and competing channels for electron-hole pair decay. The competing channels can include for example migration to non-radiative recombination centers [17]. Furthermore, VUV excitation spectra allowed to separate excitation regions for σ and π luminescence in alkali halides [30].

In the current paper, we report pioneering results of intrinsic luminescence studies in ScF_3 single crystal under synchrotron beam excitation at low temperature. The obtained luminescence characteristics will be compared with STE luminescence parameters in other trifluorides. The strong temperature quenching of STE luminescence will be demonstrated and discussed.

2. Experimental details

The nominally undoped ScF_3 single crystal has been studied by means of luminescence spectroscopy technique under VUV excitations utilizing synchrotron radiation from 1.5 GeV storage ring of MAX IV synchrotron facility (Lund, Sweden). The experiments have been carried out on the photoluminescence endstation FINESTLUMI [31, 32] of the FinEstBeAMS undulator beamline [33]. The grazing incident monochromator of SX700 type (FMB Feinwerk-ind Messtechnik GmbH (Berlin)) was applied for the monochromotization of synchrotron light. It contains the internally cooled plane mirror (M2) and two side-cooled plane gratings (PG1, 600 l/mm and PG2, 92 l/mm) intended for high and low energy ranges from 15 to 1500 eV and from 4.5 to 60 eV, respectively. In the current research, the PG2 mirror was utilized for the experiments under VUV excitations. The photon flux measured at a certain resolving power (R = 5000) was obtained of the order of 10^{13} ph/s. This value does not take into account the filters reducing the higher order of radiation. In order to suppress high orders of excitation a set of filter has been chosen. The MgF2 filter was applied for 5.50–10.8 eV energy region. At higher energies In (4*d* BE 11.5 eV), Sn (4*d* BE 23.9 eV), Mg (2*p* BE 49.6 eV) filters were used to cover almost the whole operation range of the first undulator harmonic. The excitation spectra were normalized utilizing the calibration curve obtained by means of AXUV-100G diode.

The Andor Shamrock (330i) spectrometer (0.3m) equipped with three gratings (300 l/mm, 300 nm blaze, 300 l/mm, 500 nm blaze, 1200 l/mm, 300 nm blaze) covers the spectral range 200–1500 nm. In the current research, the first grating was utilized for experiments. The Andor Shamrock spectrometer is external spectrometer and a luminescence signal is delivered to the spectrometer by means of the optical fiber. Such registration method is especially successful in case of weak luminescence signal because it allows to collect efficiently emitted photons from the samples. The exit port of the Andor Shamrock spectrometer was equipped by the Hamamatsu (H8259-00) photomultiplier covering spectral range from 200 to 700 nm. The ScF_3 single crystal was installed on the cold finger of the cryostat placed in the high vacuum chamber (10–9 mbar). The close-cycle helium cryogenic system equipped with ARS-4HW compressor (Advanced Research System) and Lake Shore temperature controller provide sample temperature in 7–400 K temperature range.

3. Results and discussion

3.1. Photoluminescence spectra

The luminescence spectrum of the ScF_3 single crystal under deep VUV excitation at low temperature (10 K) is shown in Fig. 1. The spectrum is broad and contains several overlapped emission bands. The most intensive of them is peaking at 280 nm (4.4 eV) and it is presumably attributed

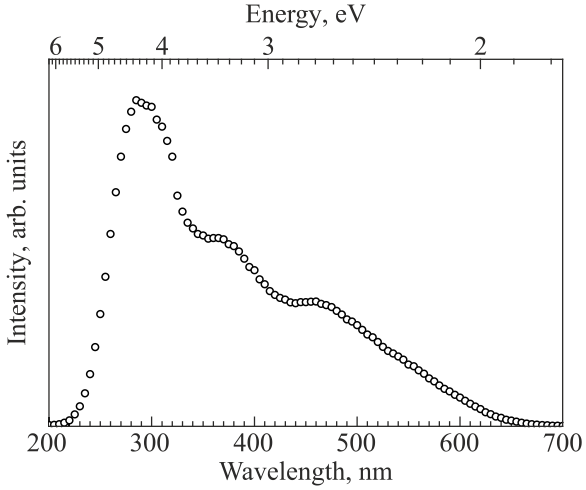

Fig. 1. The luminescence spectrum of the ScF_3 single crystal under 45 eV excitation of a synchrotron beam at 10 K.

to the radiative decay of STE in ScF_3. The less intensive emission peaks at low energies most likely belong to the extrinsic emission centers. One of the most common uncontrolled impurities in fluorides is oxygen. The spectral position of the STE emission band is similar to the corresponding emission in other trifluorides. For instance, one of the STE emission bands in YF_3 is peaking at 280 nm [17, 18], while the 300 nm band due to STE emission was observed in LaF_3 [16]. It should be also noted that the emission band due to oxygen impurity was observed in YF_3 [17] covering the spectral range from 300 nm to 600 nm. Furthermore, similar bands have been detected in other fluorides [34, 35] ascribed to oxygen related bands or *f–d* transitions of residual rare earth impurities.

3.2. Excitation spectra

The excitation spectrum of the 280 nm emission in wide excitation range (4.5–30 eV) at 10 K is show in Fig. 2.

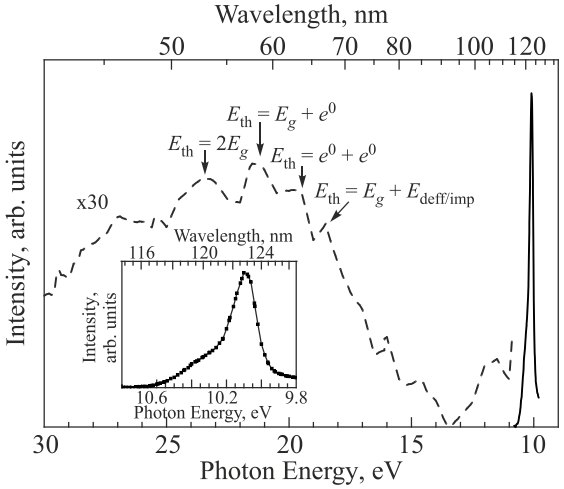

Fig. 2. The excitation spectrum of the 280 nm emission of ScF_3 single crystal at 10 K. Inset shows the low energy region of the spectra. The part of the spectrum shown by dashed line is magnified by 30 times.

The part of the excitation spectrum near excitonic and band-to-band transitions is shown in Fig. 2 inset. The excitation spectra clearly reveals the strong sharp excitation peak at about 10.1 eV. The shape of this peak is perturbed by strong absorption of excitonic transitions and therefore the excitonic peak's position can be considered as 10.2 eV. Utilizing the phenomenological approach, we can estimate the band gap value (E_g) in ScF_3 as $E_g = 1.08E_{exc}$, where E_{exc} is the energy of the excitonic transitions [36]. The band gap value is 11.02 eV and it is slightly higher than the theoretically predicted result [37]. On the other hand, the obtained band gap value is close to the value obtained before by means of resonant photoemission spectroscopy [38].

The excitation spectrum shown in Fig. 2 demonstrates that the efficiency of the excitation of the STE luminescence is very low if the excitation energy exceeds the energy of band-to-band transitions. The excitation curve at this energy range has been magnified by 30 time for better visualization (dashed line in Fig. 2). As a rule, the excitation spectrum under high-energy excitation has a complicated shape due to many factors; one of them is the process of multiplications of electronic excitations (MEE). MEE process means that two or more electron-hole pairs and, as a result, luminescence quanta are created per one absorbed photon. For a successful realization of MEE processes, the excitation energy of the photon must exceed a threshold energy $E_{th}=2E_g$. If MEE processes occur, the rise of the luminescence intensity should be observed at energies higher than E_{th} [39]. In some cases the MEE processes can be observed at energies lower than $2E_g$. It was demonstrated in [40–42] the MEE processes can be also observed if excitation energy exceeds E_{th}, which determines as follows:

$$E_{th} = E_g + e^0,$$

$$E_{th} = e^0 + e^0,$$

$$E_{th} = E_g + E_{deff/imp},$$

where e^0 is absorption energy of exciton, $E_{deff/imp}$ — absorption energy of defects or impurities.

The excitation spectrum in MEE region reveals several excitation peaks at 23.5, 21.5, 20, and 18.5 eV. Taking into account that E_g = 11.02 eV and e^0 = 10.2 eV the peaks observed in Fig. 2 demonstrate the MEE processes with different E_{th} which corresponds to the energies of $2E_g$, E_g+e^0, e^0+e^0 and $E_g+E_{deff/imp}$, respectively. However, it should be noted the E_{th} should indicates the energy of the onset of MEE processes. Therefore, the MEE excitation peaks should be slightly shifted toward high energy. It is suggested that the excitation spectrum of STE emission in high-energy range comprising the MEE region is strongly perturbed by non-raditive relaxation of hot charge carriers. Similar excitation spectra were observed for nanocrystalline phosphors [43–45] where low efficiency of the luminescence under high-energy excitations (including MEE region) was explained by the effective trapping of hot electrons and holes by surface defects, where their non-radiative relaxation occurs [43–45]. The emission spectrum (Fig. 1) demonstrates that the ScF_3 single crystal studied is not perfect, i.e., it contains a significant number of defects and extrinsic centers. We suggest that these defects and/or uncontrolled impurities can be effective trapping centers for hot electrons and holes by analogy to surface defects in nanocrystals. Whereby, the excitation spectrum in Fig. 2 (dashed line) exhibits result of the superposition of two competing processes: MEE and non-radiative relaxation processes.

3.3. Temperature dependency of luminescence

We have excluded the low wavelength emission bands from further consideration focusing attention on the STE emission band. The temperature dependency of STE emission excited in the excitonic absorption band in the ScF_3 single crystal is shown in Fig. 3. It is clearly seen that the STE emission observed significantly degrades already at 20 K and it is almost completely quenched at 50 K. The temperature quenching of luminescence intensity can be explained in the framework of the Mott–Seitz model if the radiative and non-radiative processes compete within the confines of the recombination center. Based on the Mott–Seitz model the luminescence light yield (LY) can by approximated as follows [46]:

$$\mathrm{LY} \sim \frac{1}{1 - Ce^{-\frac{E_a}{kT}}},$$

where E_a is activation energy (eV) of thermal quenching, k — Bolzman constant $8.62\cdot10^{-5}$ (eV·K^{-1}), T — temperature (K), C — constant.

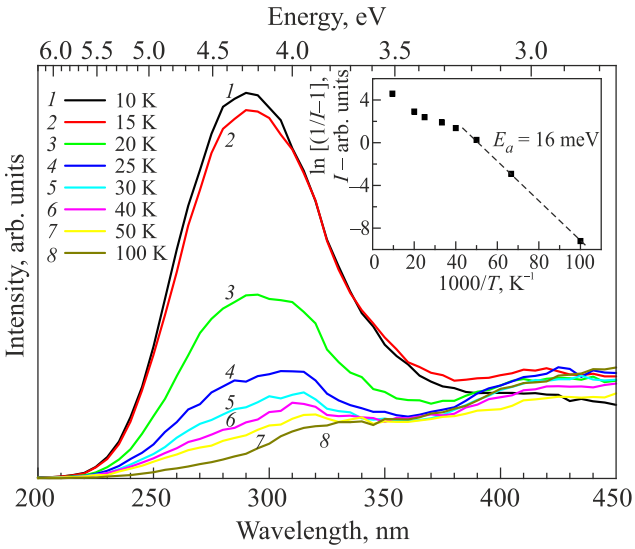

Fig. 3. (Color online) The temperature dependence of the emission spectra of ScF_3 single crystal under 10.1 eV excitation. Inset shows the temperature dependence in Mott–Seitz coordinates (see details in text).

Luminescence light yield at each temperature can be estimated as the area under emission curve of STE emission taken from Fig. 3 using Gauss deconvolution of the spectra. If one plots the function of ln [(1/LY) – 1)] versus reciprocal temperature the temperature dependence of STE emission in Mott–Seitz coordinates can be obtained as shown in the inset of Fig. 3. Using this picture the activation energy of thermal quenching can be estimated from the straight-line region (dashed line of Fig. 3 inset). The obtained value is (16 ± 2) meV, which is similar to the corresponding parameter for the STE luminescence in many other compounds [10]. However, the temperature dependence in Mott–Seitz coordinates is not straight in whole temperature range (in the inset of Fig. 3). The strong deviation from linear fit starts at temperature higher than 25 K. It means that there are extra non-radiative relaxation channels and the Mott–Seitz quenching mechanism does not work at temperatures higher than 25 K. We suggest that the high-temperature quenching of STE luminescence band can be explained by increased mobility of STE. Taking into account that the ScF_3 single crystal contains a significant number of defects and extrinsic centers, we suppose that mobile excitons at high temperature (for instance STE hopping diffusion) can be effectively trapped by crystal's imperfections where non-radiative relaxation occurs resulting to the quenching of STE emission.

4. Conclusions

Luminescence properties of the ScF_3 single crystal have been studied by means of vacuum ultraviolet excitation spectroscopy utilizing undulator synchrotron beam. The intensive broad emission band peaking at 280 nm was detected at 10 K. The analysis of the excitation spectrum as well as the temperature behavior of this emission leads us to the conclusion that this emission ordinates from the radiative decay of self-trapped exciton in ScF_3. The self-trapped exciton emission band is quenching at 50 K and the value of activation energy of 16 meV has been obtained. The self-trapped exciton emission effectively creates under direct excitation in the excitonic absorption band, whereas it is poorly excited under higher energies. Multiplication of electronic excitation processes observed in the excitation spectra of self-trapped exciton luminescence in vacuum ultraviolet spectral range are perturbed by non-radiative relaxation processes induced by the effective trapping of hot charge carriers by non-radiative centers in the ScF_3 crystal.

Acknowledgments

The work was supported by the Latvian Science Council grant LZP-2018/2-0358. The research leading to this result has also been supported by the project CALIPSO plus under the Grant Agreement 730872 from the EU Framework Programme for Research and Innovation HORIZON 2020. The author is grateful to K. Chernenko (MAX IV Laboratory, Lund University) for his assistance during beamtime experiments and to A.I. Popov for the fruitful discussions.

1. D. Karimov, I. Buchinskaya, N. Arkharova, P. Prosekov, V. Grebenev, N. Sorokin, T. Glushkova, and P. Popov, *Crystals* **9**, 371 (2019).
2. B. K. Greve, K. L. Martin, P. L. Lee, P. J. Chupas, K. W. Chapman; and A. P. Wilkinson, *J. Am. Chem. Soc*. **132**, 15496 (2010).
3. T. A. Bird, J. Woodland-Scott, L. Hu, M. T. Wharmby, J. Chen, A. L. Goodwin, and M. S. Senn, *Phys. Rev. B* **101**, 064306 (2020).
4. D. Wendt, E. Bozin, J. Neuefeind, K. Page, W. Ku, L. Wang, B. Fultz, A. V. Tkachenko, and I. A. Zaliznyak, *Sci. Adv*. **5**, 274 (2019).
5. Y. Oba, T. Tadano, R. Akashi, and S. Tsuneyuki, *Phys. Rev. Mat*. **3**, 033601 (2019).
6. L. Hu, J. Chen, A. Sanson, H. Wu, C. Guglieri Rodriguez, L. Olivi, Y. Ren, L. Fan, J. Deng, and X. Xing, *J. Am. Chem. Soc*. **138**, 8320 (2016).
7. H. Xu, R. Liu, Bo. Xu, X. Li, C. Ouyang, and S. Zhong, *New J. Chem*. **41**, 7915 (2017).
8. L. Han, Y. Wang, L. Guo, L. Zhao, and Y. Tao, *Nanoscale* **6**, 5907 (2014).
9. R. Zhu, Y. Zeng, S. Liang, Y. Zhang, Y. Qi, Y. Liu, and Y. Lyu, *J. Sol. St. Chem*. **269**, 447 (2019).
10. K. S. Song, R.T. Williams, *Self-Trapped Exciton*, Springer (1993).
11. Ch. Lushchik and A. Lushchik, *Phys. Solid State* **60**, 1487 (2018).
12. Ch. Lushchik, J. Kolk, A. Lushchik, and N. Lushchik, *Phys. Status Solidi A* **86**, 219 (1984).
13. A. Lushchik, E. Feldbach, A. Frorip, K. Ibragimov, I. Kuusmann, and Ch. Lushchik, *J. Phys.: Condens. Matter* **6**, 2357 (1994).
14. A. Lushchik, Ch. Lushchik, V. Nagirnyi, E. Shablonin, and E. Vasil'chenko, *Fiz. Nizk. Temp.* **42**, 699 (2016) [*Low Temp. Phys.* **42**, 547 (2016)].
15. A. Lushchik, Ch. Lushchik, E. Vasil'chenko, and A. I. Popov, *Fiz. Nizk. Temp*. **44**, 357 (2018) [*Low Temp. Phys*. **44**, 269 (2018)].
16. E. D. Thoma, H. Shields, Y. Zhang, B. C. McCollum, and R. T. Williams, *J. Lumin*. **71**, 93 (1997).
17. V. Pankratov, M. Kirm, and H. von Seggern, *J. Lumin*. **113**, 143 (2005).
18. V. Pankratov, M. Kirm, and H. von Seggern, *Phys. Status Solidi C* **2**, 371 (2005).
19. M. Casalboni and U. M. Grassano, *J. Phys. Chem. Solidi* **51**, 805 (1990).
20. A. P. Kozlova, V. M. Kasimova, O. A. Buzanov, K. Chernenko, K. Klementiev, and V. Pankratov, *Res. Phys.* **16**, 103002 (2020).
21. A. Tuomela, M. Zhang, M. Huttula, S. Sakirzanovas, A. Kareiva, A. I. Popov, A. P. Kozlova; A. S. Aravindh, W. Cao, and V. Pankratov, *J. Alloys Comp*. **826**, 154205 (2020).

22. L. Shirmane, V. Pankratov, and C. Feldmann, *Physica B* **504**, 80 (2017).
23. A. Kuzmanoski, V. Pankratov, and C. Feldmann, *J. Lumin*. **179**, 555 (2016).
24. A. Tuomela, V. Pankratov, A. Sarakovskis, G. Doke, L. Grinberga, S. Vielhauer, and M. Huttula, *J. Lumin*. **179**, 16 (2016).
25. V. Pankratov, V. Osinniy, A. Nylandsted Larsen, and B. Bech Nielsen, *Phys. Rev. B* **83**, 045308 (2011).
26. A. Shalaev, R. Shendrik, A. Rusakov, A. Bogdanov, V. Pankratov, K. Chernenko, and A. Myasnikova, *Nucl. Inst. Meth. B* **467**, 17 (2020).
27. A. I. Popov, L. Shirmane, V. Pankratov, A. Kotlov, A. Lushchik, V. E. Serga, L. D. Kulikova, G. Chikvaidze, and J. Zimmermann, *Nucl. Inst. Meth. B* **310**, 23 (2013).
28. P. V. Savchyn, V. V. Vistovskyy, A. S. Pushak, A. S. Voloshinovskii, A. V. Gektin, V. Pankratov, and A. I. Popov, *Nucl. Inst. Meth*. **274**, 78 (2012).
29. J. H. Beaumont, A. J. Bourdillon, and M. N. Kaber, *J. Phys. C* **9**, 2961 (1976).
30. M. Yanagihara, Y. Kondo, and H. Kanzaki, *J. Phys. Soc. Jpn*. **52**, 4397 (1983).
31. V. Pankratov and A. Kotlov, *Nucl. Inst. Meth. Phys. Res. B* **474**, 35 (2020).
32. V. Pankratov, R. Pärna, M. Kirm, V. Nagirnyi, E. Nommiste, S. Omelkov, S. Vielhauer, K. Chernenko, L. Leisberg, P. Turunen, A. Kivimäki, E. Kukk, M. Valden, and M. Huttula, *Rad. Measur*. **121**, 91 (2019).
33. R. Pärna, R. Sankari, E. Kukk, E. Nommiste, M. Valden, M. Lastusaari, K. Kooser, M. Hirsimäki, S. Urpelainen, P. Turunen, A. Kivimäki, V. Pankratov, L. Reisberg, F. Hennies, H. Tarawneh, R. Nyholm, and M. Huttula, *Nucl. Inst. Meth. A* **859**, 83 (2017).
34. C. Feldmann, T. Justel, C. R. Ronda, and D. U. Wiechert, *J. Lumin*. **92**, 245 (2001).
35. J.C. Krupa and M. Queffelec, *J. Alloys Comp*. **250**, 287 (1997).
36. P. Dorenbos, *Opt. Mater*. **69**, 8 (2017).
37. D. Bocharov, P. Žgun, S. Piskunov, A. Kuzmin, and J. Purans, *Fiz. Nizk. Temp*. **42**, 710 (2016) [*Low Temp. Phys*. **42**, 556 (2016)].
38. M. Umeda, Y. Tezuka, S. Shin, and A. Yagishita, *Phys. Rev. B* **53**, 1783 (1996).
39. E. R Ilmas, G. G. Liidya, and Ch. B. Lushchik, *Opt. Spektroskop.* **18**, 453 (1965).
40. A. Lushchik, E. Feldbach, R. Kink, Ch. Lushchik, M. Kirm, and I. Martinson, *Phys. Rev. B* **53**, 5379 (1996).
41. E. Feldbach, M. Kamada, M. Kirm, A. Lushchik, Ch. Lushchik, and I. Martinson, *Phys. Rev. B* **56**, 13908 (1997).
42. A. Lushchik, Ch. Lushchik, P. Liblik, A. Maaroos, V. N. Makhov, F. Savikhin, and E. Vasil'chenko, *J. Lumin*. **129**, 1894 (2009).
43. L. Shirmane and V. Pankratov, *Phys. Status Solidi* (*RRL*) **10**, 475 (2016).
44. V. Pankratov, S. Chernov, L. Grigorjeva, T. Chudoba, and W. Lojkowski, *IEEE Trans. Nucl. Sci*. **55**, 1509 (2008).
45. V. Pankratov, A. I. Popov, L. Shirmane, A. Kotlov, and C. Feldmann, *J. Appl. Phys*. **110**, 053522 (2011).
46. V. Pankratov, L. Grigorjeva, D. Millers, and H. M. Yochum, *Phys. Status Solidi C* **4**, 801 (2007).

Низькотемпературна люмінесценція монокристалів ScF_3 під впливом вакуумних ультрафіолетових збуджень синхротронним пучком

В. Панкратова, В. Панкратов

Виміряно фотолюмінесценцію та спектри збудження монокристалів ScF_3 при вакуумних ультрафіолетових збудженнях під впливом ондуляторного синхротронного випромінювання кільцевого накопичувача 1,5 ГеВ синхротрона MAX IV. Пік емісії при 280 нм пояснюється емісійною смугою екситонів у ScF_3, які автолокалізовані. Встановлено, що ця емісія загасає при 50 К. Отримано енергію активації температурного згасання. Спектри збудження в вакуумному ультрафіолетовому діапазоні вказують на те, що люмінесценція автолокалізованих екситонів ефективна при прямому порушенні в смузі екситонного поглинання, а при більш високих енергіях їх збудження сильно пригнічуються, але множення процесів електронного збудження успішно ідентифікується.

Ключові слова: ScF_3, VUV люмінесцентна спектроскопія, синхротронне випромінювання.

Institute of Solid State Physics, University of Latvia as the Center of Excellence has received funding from the European Union's Horizon 2020 Framework Programme H2020-WIDESPREAD-01-2016-2017-TeamingPhase2 under grant agreement No. 739508, project CAMART²